32nd URSI GASS, Montreal, 19-26 August 2017

Observations of 5.9 GHz radio wave propagation and 802.11p network performance at road junctions

C.J. Clayton(1), A.J. Stocker*(1), D. Hassan(1), T. Edwards(2), and D. Mearns(2)
(1) University of Leicester, Leicester, U.K.
(2) HORIBA MIRA Ltd, U.K.

Abstract

The propagation of 5.9 GHz radio signals and performance of an 802.11p network was investigated at three road junctions. The range below which acceptable network performance occurs is greater (~25 m) at junctions with few buildings than those with many buildings (~15–20 m).

1. Introduction

Vehicle-to-vehicle (V2V) and vehicle-to-infrastructure (V2I) communications (collectively known as V2X) are important components of drive towards connected and autonomous vehicles. The performance of such systems (e.g. IEEE 801.11p) depends on the propagation environment, for example in motorway driving the propagation path is relatively uncluttered and ranges are many hundreds of metres (e.g. see [1]), while in the urban environment, the range will typically be much shorter (10s of metres) because of the presence of buildings (e.g. see [2]). Some of the propagation modes that can occur in the urban environment are illustrated in Figure 1. For safety critical systems (e.g. collision avoidance), the shorter propagation ranges result in shorter timescales for drivers (human or machine) to react. Mangel et al., [2] did an extensive survey of the effect of a number of junctions and developed a model (virtualsource11p) to predict the signal path loss.

In this paper, experimental measurements of radio propagation effects and network performance of a 802.11p system for three junctions with different building densities are presented. These are then compared with the predictions from virtualsource11p [2].

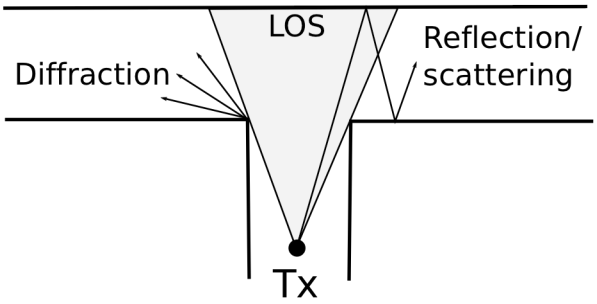

Figure 1. A schematic of the likely propagation modes found in the urban environment.

2. Method

A measurement system similar to that used by [3] consisting of an 802.11p network system (NS) and a continuous wave system (CWS) was used to simultaneously measure network performance and channel parameters (signal strength and Doppler frequency), respectively at three road T-junctions (Junction A was built-up, Junction B was partially built-up, and Junction C was open). The antennas for the CWS and NS were a distance of 0.508 m apart (corresponding to ten wavelengths at 5.9 GHz) and a height of 1m. While, this offset between the antennas means that the propagation path for the CWS signal is slightly different to that of the NS signals, systematic differences in measurements were small compared to the fading level.

The CWS used a signal generator to produce a 5.9 GHz CW signal with a power of 16 dBm. The transmitter and receiver used omnidirectional antennas with a gain of 6 dBi. The spectrum of the received signal was measured every 1.5 s over a range of 500 Hz (centred on the carrier) which meant that the Doppler shifts and spreads caused by traffic (up to speeds of approximately 13 ms^{-1}) could be measured. Two example spectra are presented in Figure 2. From these spectra, the peak power and the Doppler spread can be derived. Thirty spectra were

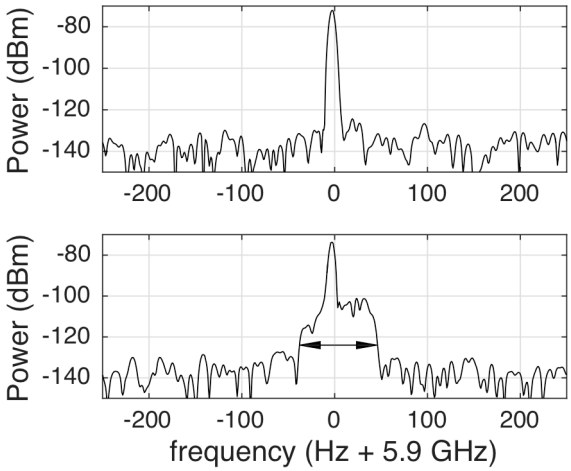

Figure 2. Two spectra obtained at a distance of +8 m from Junction A. In the bottom panel, a passing vehicle (travelling at ~3 ms^{-1}) affects the spectrum. The arrows indicate the Doppler spread.

collected at each location allowing mean values of peak signal strength and Doppler spread to be derived as a function of position.

The NS consisted of two NEC Linkbirds (version 4), one operating as a transmitter and the other as a receiver with identical power and antennas to the CWS. A packet, which consisted of a time stamp, a unique packet number, and a collection of random numbers with a checksum, was emitted by the transmitter every 0.1 s. The time that each packet arrived at the receiver was recorded along with the RSSI. However, the clocks at the transmitter and receiver were not synchronised and this meant that the delay time could not be reliably determined (given that this was a single hop link, this is not likely to have varied much in any case). While the RSSI of the NS could be used to measure the signal strength, there was a systematic difference between the values obtained by the two systems and the calibrated CWS is likely to produce a more accurate measurement and be able to detect the signal at times when it was too weak to allow successful reception of the packets.

For each junction, the transmitter was fixed in position and measurements collected by the stationary receiver at various distances, d_r from the centre of the junction separated by fixed intervals (Δd). A laser-rangefinder was used to determine the location of the systems relative to a fixed reference point (the nominal centre of each junction) with an accuracy of ±0.5 mm. For Junction A, Δd =1 m, while for Junctions B and C, Δd=0.2 m. The separation between measurement points (Δd) was a compromise between practicality (i.e. the time taken) and the distance resolution. For each location, the mean peak power (MPP) was derived from the 30 spectra obtained, together with a single value of the packet delivery ratio (PDR, i.e. the fraction of transmitted packets successfully received).

3. Results

3.1 Junction A

Junction A is relatively built-up with buildings located along all roadsides (Figure 3). However, the junction is asymmetric in terms of buildings since it is more open in the positive d_r direction (e.g. the Library Podium is an open space on a raised platform with 1.68 m high walls).

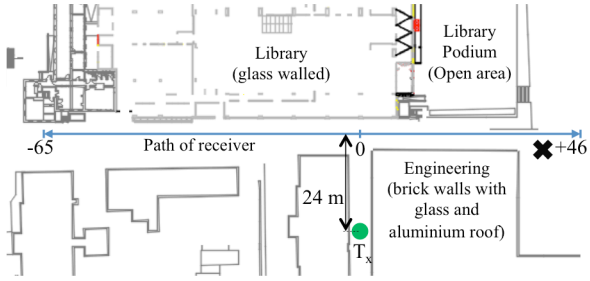

Figure 3. Map of Junction A indicating the location of the transmitter and the path of the receiver.

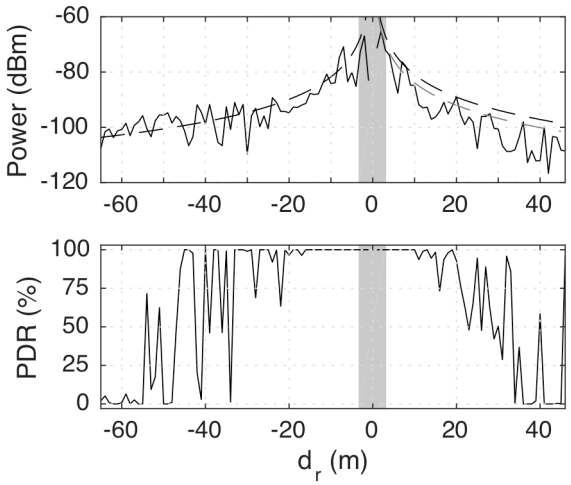

Figure 4. Plot of (top panel) Mean peak signal power and (bottom panel) PDR as a function of distance from the intersection for Junction A. The dashed lines are the virtualsource11p predictions of the power for urban (black) and sub-urban (grey) cases. The shaded area represents where a LOS path is present.

The transmitter was placed in the centre of a 4.7 m wide street canyon a distance 24 m from the junction, while the receiver moved along the middle of the road either side of the T-junction from -65 m to 46 m.

The observed MPP and PDR as a function of d_r averaged over six runs are presented in Figure 4. As expected, both the MPP and PDR are high in the LOS region at the centre of the intersection and then decrease with increasing $|d_r|$. The MPP exhibits fading (of up to 10 dB) even in the LOS region, demonstrating the presence of multipath propagation (error bars have been omitted for clarity – the median inter-decile range is 4 dB). The reduction in MPP and PDR occurs closer to the junction in the positive d_r direction than for negative d_r. This may result from the asymmetry in the presence of buildings either side of the junction since there are buildings both sides of the road at negative d_r that will reflect the radio waves and extend the coverage range, while at positive d, there is a building on only one side of the road when d_r>10 m, and this will reduce the number of reflections and hence the signal strength. The values of power derived from the virtualsource11p model are a close fit to the observations for d_r<0, while for dr>0, they overestimate the measured signal level by 5–10 dB. From the measurements of PDR, three regions can be identified. From -20<d_r<10 m, the network operates with close to 100% reliability, for d_r<-55 and d_r>40 m, the network operates with close to 0% reliability (although for some positions the PDR is higher than this), while a transition region with strongly varying in PDR lies between these two cases.

3.2 Junction B

Junction B is a less-built up area than Junction A (Figure 5) since buildings were not present on both sides

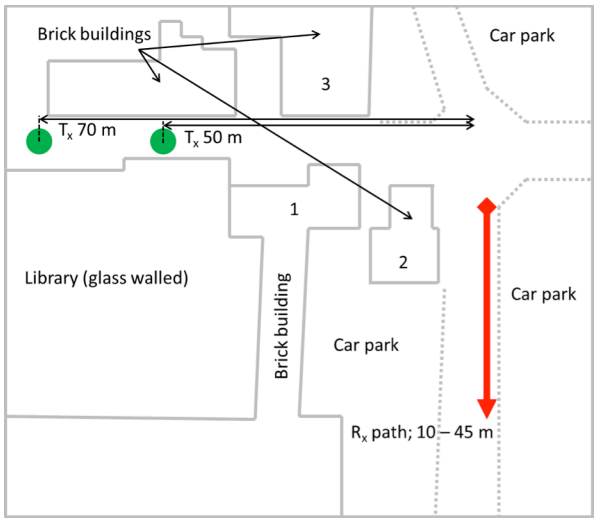

Figure 5. Map of Junction B

of the road. While the transmitter was placed in a street canyon, the road along which the receiver was moved had buildings on one side and an open area (car park) lined with a hedge on the other. While two sets of measurements were made, with the transmitter 50 m (Tx50) and 70 m (Tx70) away from the intersection centre, only the former will be presented here. Since it was not possible to conduct measurements at d_r<10 m, the geometry meant that NLOS conditions were present throughout.

The observations of MPP and PDR for Tx50 are presented in Figure 6. As expected, the signal strength tends to decrease with increasing d_r, although both spatial and temporal fading is of the order of 10 dB and there are peaks in the signal that are not well related to any clear changes in the propagation path (e.g. at d_r~30 m, although this may be related to the path clearing the corner of Building 2). The predictions of signal power made by virtualsource11p are about 20 dB higher than the measured values. The PDR is essentially 0% for d_r>15 m, but there are some instances where PDR non-zero. This is related to the presence of vehicles providing a reflecting

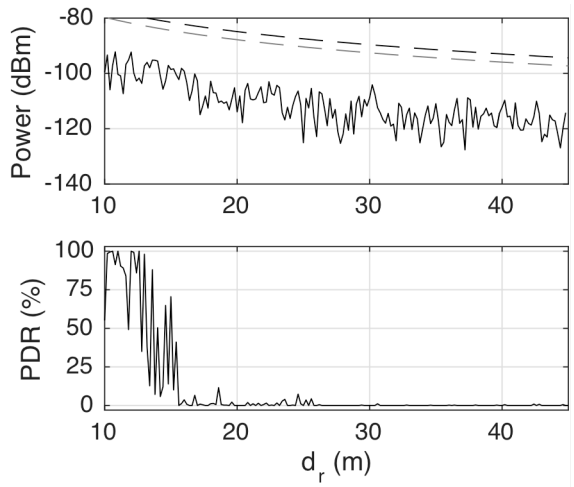

Figure 6. As for Figure 4, except for Junction B. Note that propagation was non-LOS at all distances.

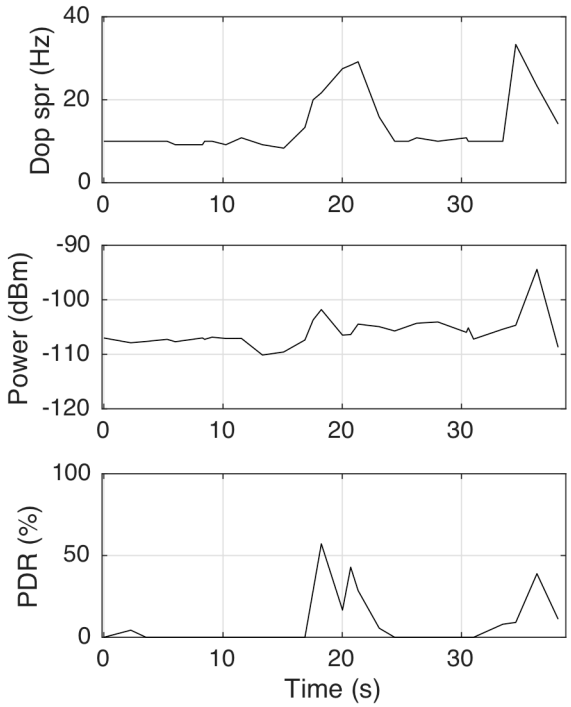

Figure 7. Plot of (from top to bottom) Doppler Spread, peak power, and PDR as a function of time at d_r=24.6 m from Junction B. The PDR is calculated per spectrum (i.e. based on ~15 packets in 1.5 s)

or scattering path for the signals. An example is presented in Figure 7, where two vehicles caused a simultaneous increase in Doppler spread, PDR, and (to a lesser extent) in signal strength at t=15–25 s and t=32 s onwards.

3.3 Junction C

The layout of Junction C together with the location of the transmitter and paths taken by the receiver are presented in Figure 8. The transmitter was fixed at the centre of a four-lane road at a distance of 46 m from the mid-point of the intersection. Measurements were taken along the sides of the road 5 m from the centre on the same side as the transmitter (i.e. adjacent to) and 8 m from the centre on the opposite side with Δd=0.2 m. This junction is open compared to the others with a building present only to one side (i.e. there were no street canyons). There was a mix

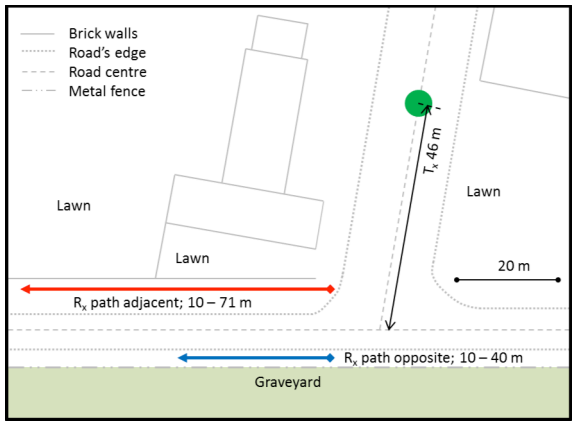

Figure 8. Map of Junction C

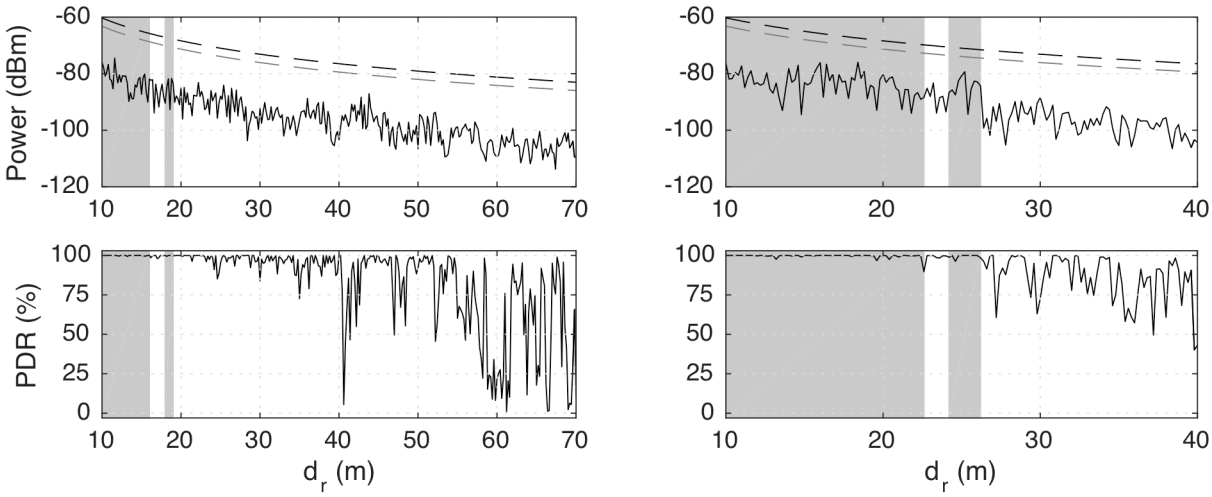

Figure 9. As for Figure 4, except for Junction C, (left hand column) same side of the road as and (right hand) opposite side of the road to the transmitter.

of LOS and NLOS conditions on both paths with data being collected over 10 m into the NLOS region in the opposite path and over 50 m into the NLOS region of the adjacent path. A road sign blocks the visible LOS when d~25 m (for the opposite path) and just under 20 m (for the adjacent path), although the plastic construction of the sign means that it has no measureable effect on the radio propagation or network performance.

The PDR and MPP for the data collected on the opposite and adjacent paths are presented in Figure 9. As expected, there is a gradual decline in signal strength as d_r increases while, as for Junction B, the virtualsource11p predictions exceed the measurements by about 20 dB. Perhaps less expected, is that there appears to be little difference between LOS and NLOS conditions except at around 25 m for the path on the opposite side of the road. For both the adjacent and opposite paths, the PDR is close to 100% for d<25 m and between 80–100% for 25<d<40 m. For d>40 m the PDR varies between 0 and close to 100%. Since this is a wider junction than Junctions A and B, the signal levels are higher and the network performance is better.

4. Concluding remarks

Measurements of signal strength and network performance have been made at three road junctions that differed in how built-up they were. For a junction with buildings on all sides of the road, the predictions of signal strength from virtualsource11p are consistent with the observations. However, for more open junctions (e.g. with no buildings along one side of the road), virtualsource11p underestimates the loss by about 20 dB probably because of the reduction in the number of reflected signals arriving at the receiver. The range over which an 802.11p network provides reliable service also depends on the type of junction being about 20 m for a built-up junction, and upwards of 25 m for a very open junction.

5. References

1. A. Paier, R. Tresch, A. Alonso, D. Smely, P. Meckel, Y. Zhou, and N. Czink, "Average downstream performance of measured IEEE 802.11p infrastructure-to-vehicle links", in *IEEE International Conference on Communications, Workshop on Vehicular Connectivity*, Cape Town, South Africa, May 2010.

2. T. Mangel, O. Klemp, and H. Hartenstein, "5.9 GHz inter-vehicle communication at intersections: a validated non-line-of-sight path-loss and fading model", EURASIP Journal on Wireless Communications and Networking, 2011, 2001:182.

3. L. Cheng, B. Henty, D.D. Stancil, F. Bai, and P. Mudalige, "A fully mobile, GPS enabled, vehicle-to-vehicle measurement platform for characterization of the 5.9 GHz DSRC channel", *In IEEE Antennas and Propagation Society, AP-S International Symposium (Digest)*. pp. 2005–2008, 2007.